Vibration Reduction of Wind Turbines Using Tuned Liquid Column Damper Using Stochastic Analysis

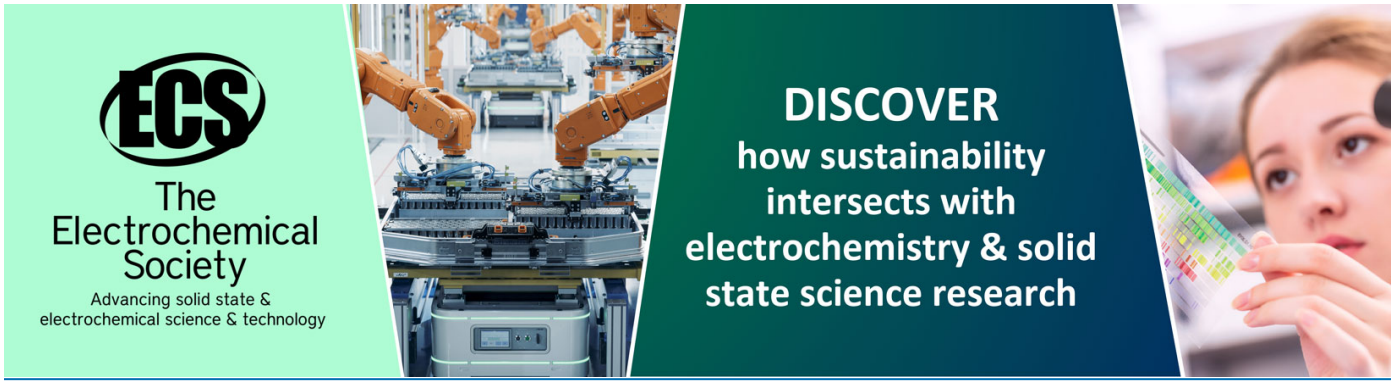

Vibration Reduction of Wind Turbines Using Tuned Liquid Column Damper Using Stochastic Analysis

M H Alkmim[1], M V G de Morais[1], A T Fabro[1]

[1] Departament of Mechanical Engineering, University of Brasilia, Campus Universitario Darcy Ribeiro, Brasilia, 70910-900, Brazil

E-mail: mansour.alk@gmail.com

Abstract. Passive energy dissipation systems encompass a range of materials and devices for enhancing damping. They can be used both for natural hazard mitigation and for rehabilitation of aging or deficient structures. Among the current passive energy dissipation systems, tuned liquid column damper (TLCD), a class of passive control that utilizes liquid in a "U" shape reservoir to control structural vibration of the primary system, has been widely researched in a variety of applications. This paper focus in TLCD application for wind turbines presenting the mathematical model as well as the methods used to overcome the nonlinearity embedded in the system. Optimization methods are used to determine optimum parameters of the system. Additionally, a comparative analysis is done considering the equivalent linearized system and the nonlinear system under random excitation with the goal of compare the nonlinear model with the linear equivalent and investigated the effectiveness of the TLCD. The results are shown using two types of random excitation, a white noise and a first order filters spectrum, the latter presents more satisfactory results since the excitation spectrum is physically more realistic than white noise spectrum model. The results indicate that TLCDs at optimal tuning can significantly dissipate energy of the primary structure between 3 to 11%.

1. Introduction

The current brazilian energy scenario undergoes a delicate situation, the recent 2015 crisis in the energy sector made the ONS (National System Organ) approve the return of thermal power plants. According to data released by the PNE 2030 (National Energy Plan) most of the energy produced in the country comes from hydroelectric plants and it is anticipated that by the year 2030, hydroelectric plants will have participation of 77.4 % of the energy matrix [1]. For all of its merits, there are uncertainties regarding its offer in the future. Major projects such as S. Luiz do Tapajos and Belo Monte have faced serious socio-environmental conflicts such as the transposition of rivers, impacts on fauna and conflicts with local communities. Other strategic issues of hydropower is that there is a high dependence on weather conditions and the location of the energy which is primarily in the Amazon region. Recent examples of mismanagement of water levels in reservoirs lead in the reactivation of fossil fuel based power plants that generate environmental and economic damage.

Given these facts, the government has announced strategical plans to change the current state and diversify its electricity sources. One of the proposed options is wind energy, which currently accounts for a small portion of the energy matrix and holds enormous potential. It is expected that the country will have more than 17 GW of wind power by 2022 according to PDE-2022

(Ten Year Plan for Energy Expansion). In the current scenario, the installed capacity of wind power produces a total of 6.1 GW, a figure far below the production capacity according to the Atlas of the wind potential which is around 143.5 GW [1].

Remarkable progress in the technology used in wind turbines has been made over the past years; advances in the field of structural and dynamic analysis allow the creation of larger and more efficient wind turbines. However, higher and slender structures poses challenges concerning its integrity in relation to the dynamic loads from wind, ocean waves or earthquakes. Serious efforts have been undertaken to develop the concept of vibration control of wind turbines.

Vibration control has raised various technical studies in recent years [2–5]. Additionally, different types of devices have encounter vibration control applications in wind turbines [5–7]. In particular, among the energy dissipation systems, Tuned Liquid Column Dampers (TLCDs) are emerging in several specialized publications and has become a good option due to its relatively low cost and good efficiency.

As shown in Figure 1, the TLCD operates based on the movement of the liquid column. The column may have different geometries, particularly in this paper, the TLCD has a "U" shape. The TLCD requires no extra mechanism such as springs or joints, besides that, its geometry may vary according to design needs, making them very versatile devices. While the apparent simplicity of the system, the damping is dependent on the amplitude of the liquid, and therefore the dynamics of TLCD is nonlinear which brings some mathematical complications to the model.

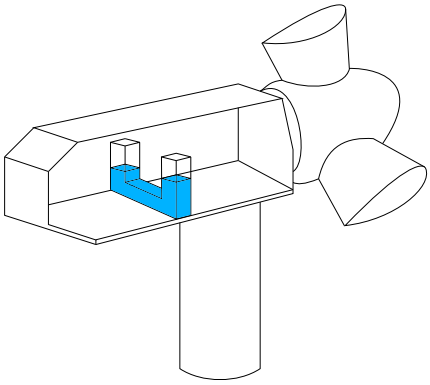

Figure 1: Possible tuned liquid column damper scheme applied in wind turbine.

In this work, a comparative analysis is done considering the nonlinear and equivalent linearized system when subject to two types of random excitation, white noise and first order filter spectrum. Section 2 presents the TLCD and structure modelling as well as the optimum TLCD parameters under random excitation using statistical linearization. Section 3 presents the response due to random excitation using PSD and direct integration schemes. Section 4 shows some numerical results obtained from a wind turbine case study. And, finally, section 5 draws some conclusion and final remarks.

2. TLCD and structure modelling

Consider the TLCD model mounted structure as sketched in Figure 2. The idealization for the structure is acceptable because the support has negligible mass and constant cross section, thus, it is possible to approach the shear-frame system as a one degree of freedom model with stiffness and equivalent damping.

The equation describing the motion of the fluid is given by

$$\rho A l\ddot{u}(t) + \frac{1}{2}\rho A\xi|\dot{u}(t)|\dot{u}(t) + 2\rho A g u(t) = -\rho A b\ddot{x}(t), \tag{1}$$

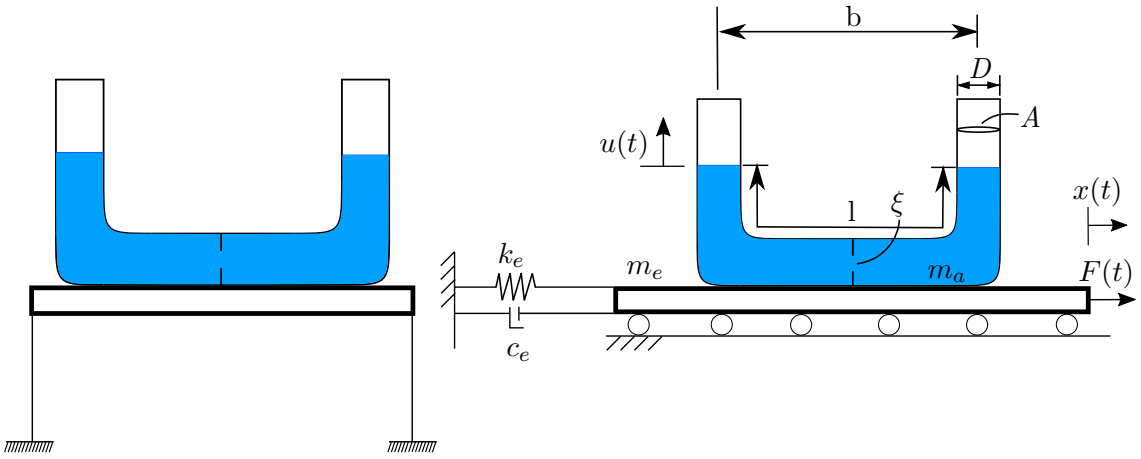

Figure 2: Schematic model of the system.

where $u(t)$ is the displacement of fluid function, $x(t)$ is the displacement of the primary system function, ρ is the fluid density, ξ is the head loss coefficient, A is the cross section area of the column, b and l are the horizontal and total length of the column respectively and g is the gravity constant. It can be observed that the TLCD mass is given by $m_a = \rho A l$, the TLCD damping is $c_a = \frac{1}{2}\rho A \xi |\dot{u}(t)|$ and the TLCD stiffness is given by $k_a = \rho A g$. The natural frequency of oscillation in the tube can be obtained by $\omega_a = \sqrt{2g/l}$.

The equation of motion of the primary structure is given by

$$(m_e + m_a)\ddot{x}(t) + \rho A b \ddot{u}(t) + c_e \dot{x}(t) + k_e x(t) = F(t), \tag{2}$$

where the parameter m_e is the structure mass, k_e the structure stiffness, c_e the structure damping and $F(t)$ the external force. Thus, combining (1) and (2). The equation of motion in matrix form can be written as

$$\begin{bmatrix} m_e + m_a & \alpha m_a \\ \alpha m_a & m_a \end{bmatrix} \begin{Bmatrix} \ddot{x} \\ \ddot{u} \end{Bmatrix} + \begin{bmatrix} c_e & 0 \\ 0 & c_a \end{bmatrix} \begin{Bmatrix} \dot{x} \\ \dot{u} \end{Bmatrix} + \begin{bmatrix} k_e & 0 \\ 0 & k_a \end{bmatrix} \begin{Bmatrix} x \\ u \end{Bmatrix} = \begin{Bmatrix} F(t) \\ 0 \end{Bmatrix} \qquad |u| \leqslant \frac{l-b}{2}, \tag{3}$$

where $\alpha = b/l$ is the dimensionless length ratio. The condition presented at (3) is needed to ensure that the liquid in the column do not spill water and consequently change its damping characteristic. Equation (3) can also be written with the mass matrix in its dimensionless form, given by

$$\begin{bmatrix} 1+\mu & \alpha\mu \\ \alpha & 1 \end{bmatrix} \begin{Bmatrix} \ddot{x} \\ \ddot{u} \end{Bmatrix} + \begin{bmatrix} 2\omega_e\zeta_e & 0 \\ 0 & \frac{\xi|\dot{u}|}{2l} \end{bmatrix} \begin{Bmatrix} \dot{x} \\ \dot{u} \end{Bmatrix} + \begin{bmatrix} \omega_e^2 & 0 \\ 0 & \omega_a^2 \end{bmatrix} \begin{Bmatrix} x \\ u \end{Bmatrix} = \begin{Bmatrix} \frac{F(t)}{m_e} \\ 0 \end{Bmatrix}, \tag{4}$$

where ζ_e and ω_e are the damping ratio and natural frequency of the structure, respectively. The dimensionless parameters mass ratio μ and tuning ratio γ are defined as

$$\mu = \frac{m_a}{m_e}; \qquad \gamma = \frac{\omega_a}{\omega_e}. \tag{5}$$

2.1. Statistical Linearization

The nonlinear nature of the damping requires the determination of a equivalent value to the damping coefficient. Roberts and Spanos [8] proposed a procedure to estimate the optimum value of the damping coefficient utilizing statistical linearization method. It is possible to express the

error between the nonlinear system with the equivalent linear system as $\epsilon = (1/2)\rho A\xi|\dot{u}|\dot{u} - c_{eq}\dot{u}$, where the value of the equivalent damping c_{eq} can be obtained by minimizing the standard deviation of the error value, namely $E\{\epsilon^2\}$. Assuming that the liquid velocity has Gaussian form, the expression for the equivalent damping is given as

$$c_{eq} = \sqrt{\frac{2}{\pi}}\rho A\xi\sigma_{\dot{u}} = 2\omega_a\zeta_a, \tag{6}$$

where $\sigma_{\dot{u}}$ is the standard deviation of the fluid velocity. Therefore, the equivalent damping approached by statistical linearization c_{eq} can replace the nonlinear value c_a in (3). The equivalent damping can also be expressed as a function of the absorber damping ratio ζ_a in order to make the optimization calculation more convenient.

2.2. Optimum parameters

To find the optimized absorber damping ratio and optimized tuning ratio we applied the method proposed by Yalla and Kareem [9]. First, we define the system linearized frequency response function of the first and second degree of freedom as $H(\omega) = X(\omega)/F(\omega)$ and $G(\omega) = U(\omega)/F(\omega)$ respectively. The system responses can be calculated such that the variance of the main system and TLCD velocity are obtained by [10]

$$\sigma_x^2 = \int_{-\infty}^{\infty} |H(\omega)|^2 S_{ff}(\omega)d\omega, \qquad \sigma_{\dot{u}}^2 = \int_{-\infty}^{\infty} \omega^2|G(\omega)|^2 S_{ff}(\omega)d\omega, \tag{7}$$

wherein $S_{ff}(\omega)$ is the power spectral density (PSD) of the input force and can assume different values depending on the wind profile model chosen. The solution of the complex integrals at (7) needs a simplified approach to be solved [8].

For white noise excitation, particularly, it is possible to obtain a closed-form solution. The optimal conditions are given by

$$\frac{\partial\sigma_{\dot{u}}^2}{\partial\zeta_a} = 0, \quad \frac{\partial\sigma_x^2}{\partial\gamma} = 0, \tag{8}$$

the solutions for the case of undamped primary system ($\zeta_e = 0$) are

$$\zeta_{opt} = \frac{\alpha}{2}\sqrt{\frac{2\mu\left(\alpha^2\frac{\mu}{4} - \mu - 1\right)}{(\alpha^2\mu^2 + \alpha^2\mu - 4\mu - 2\mu^2 - 2)}}, \tag{9}$$

$$\gamma_{opt} = \frac{\sqrt{1 + \mu(1 - \frac{\alpha^2}{2})}}{1 + \mu}, \tag{10}$$

where the values obtained are functions of system parameters such as mass, natural frequency and the length of the tube.

Figure 3 illustrates the variation of parameters ζ and γ with the variation of the mass ratio μ and the length ratio α. Analyzing Figure 3(a), the damping ratio increases for larger values of μ. This means that the bigger the TLCD is, the greater the damping ratio will be which confirm the prediction from (9). On the other hand, in Figure 3(b), the tuning ratio decreases as the mass ratio increases. The geometric parameter α shows that for TLCDs with no vertical lengths, i.e. $\alpha = 1$, the value of damping ratio is greater although its shape change considerably and the TLCD ends functioning purely as a sloshing damper. This observation can be physically understood by the fact that there is more mass in the horizontal portion of the TLCD which

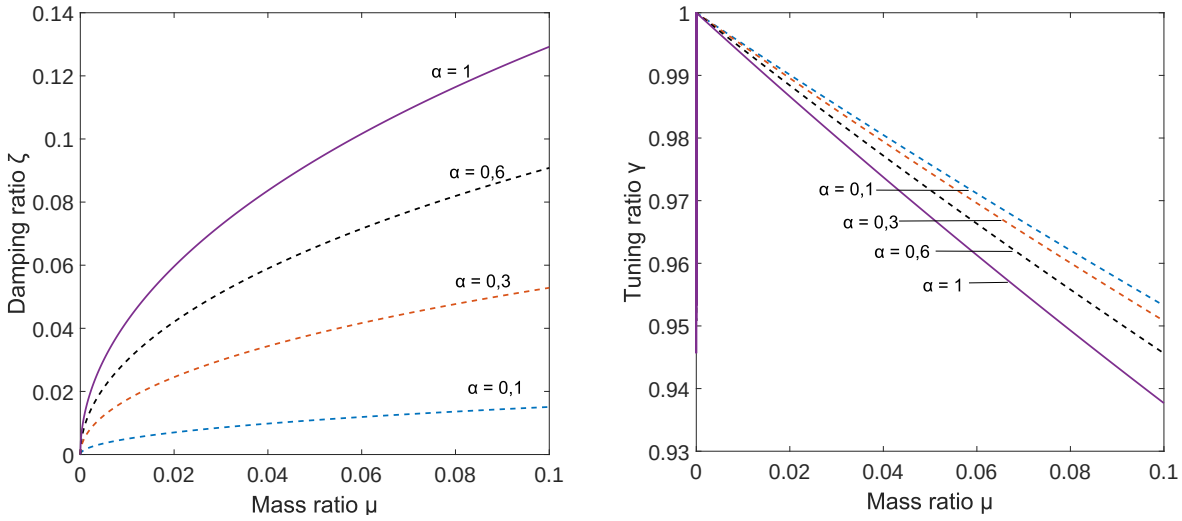

Figure 3: Comparing the optimized parameters (a) ζ and (b) γ for different values of the variables μ and α.

indirectly contributes to the sloshing damper. Larger values α make the tuning ratio decrease, however this variation is less significant than the change in mass ratio.

White noise is a type of power spectral density function (PSD) idealization that covers all frequency bands. It is used to simplify the analysis so that it is possible to obtain satisfactory initial results. The forcing function as a filter of first order (FOF) can be used to approximate wind-induced positive pressures along wind loading. Other types of PSD are worth mentioning such as the Spectrum Kanai-Tajimi and the Spectrum of Davenport both produce time series of physically representative winds by taking into consideration aspects of relevance to the real problem like roughness, heights, wind forces and general changes the dynamic properties of excitement. Table 1 shows usual power spectral density functions for modeling the wind.

Table 1: Usual power spectral density functions for modeling the wind.

Filter	Power spectral density functions
White Noise	$S_{WN}(\omega) = S_0$
First Order Filter	$S_{FOF}(\omega) = S_0/(\nu^2 + \omega^2)$
Davenport Filter	$S_{DAV}(\omega) = 4\kappa LU\chi/(1+\chi^2)^{4/3}, \quad \chi = \omega L/U$
Kanai-Tajimi Filter	$S_{KT}(\omega) = (1 + 4\xi_g^2(\omega/\omega_g)S_0)/[1 + (\omega/\omega_g)^2 + 4\xi_g^2(\omega/\omega_g)^2]$

For the first order filter, S_0 is the power spectral density for the case of white noise, ν is a filter parameter and ω is the frequency of the oscillating system. For Davenport filter, ω is the frequency, U is the average velocity, L is the length and κ is the drag coefficient [11]. For Kanai-Tajimi filter, ω_g and ξ_g can be interpreted as characteristic frequency and characteristic damping ratio respectively. The Kanai-Tajimi spectrum amplifies the frequency around ω_g where it attenuates high frequencies and have minimal effect on small frequencies [12]. The analysis

in this paper will be limited to white noise and the first order filter.

Figure 4 illustrates the First Order Filter (FOF) PSD for different values of the parameter ν and the frequency response function of the primary system for reference. It can be shown that for high values of ν the FOF PSD can be simplify to the white noise PSD.

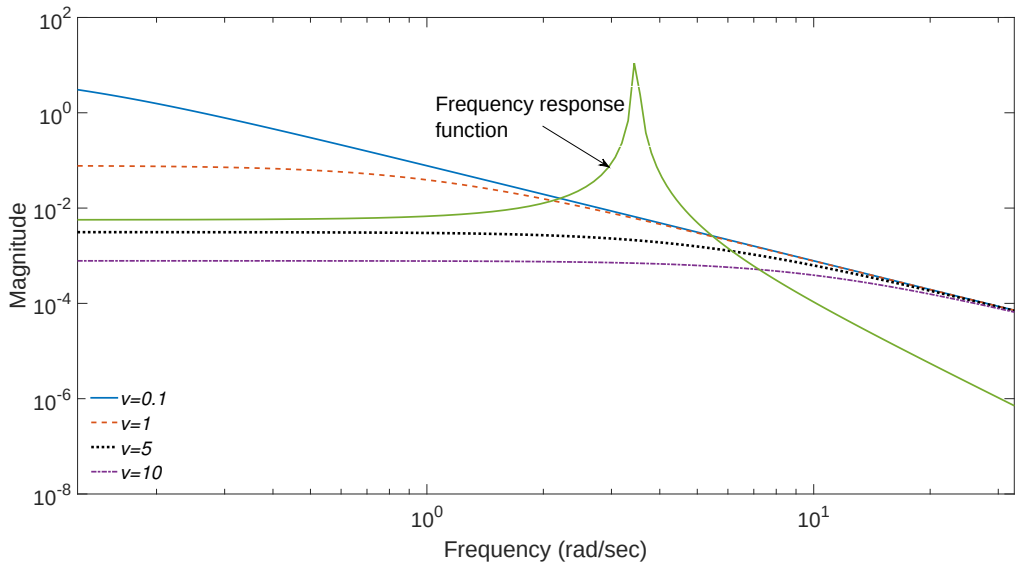

Figure 4: FOF in m for different values of ν and frequency response function in m/s^2 of the primary system.

Table 2 and Table 3 show optimized values for damping ratio and tuning for the white noise and FOF PSDs considering different damping conditions of the primary system and different values of the mass ratio. For the both PSDs it was used $\alpha = 0.9$ and for the FOF, $\nu = 0.1$.

Table 2: Optimized absorber parameters for white noise noise for different mass ratio and primary system damping

μ (%)	Primary system without damping		Damping of 1%		Damping of 2%		Damping of 5%	
	γ_{opt}	ζ_{opt}	γ_{opt}	ζ_{opt}	γ_{opt}	ζ_{opt}	γ_{opt}	ζ_{opt}
0.5	0.9965	0.0318	0.9962	0.0318	0.9959	0.0318	0.9949	0.0318
1.0	0.9930	0.0448	0.9926	0.0448	0.9922	0.0448	0.9908	0.0448
1.5	0.9896	0.0548	0.9891	0.0548	0.9885	0.0548	0.9869	0.0548
2.0	0.9862	0.0631	0.9856	0.0631	0.9850	0.0631	0.9832	0.0631

It can be noted from Table 2 and Table 3 that values for ζ_{opt} are very similar for both PSDs. Additionally, the impact of the primary system damping is more sensitive when the excitement is described by a first order system (FOF). The tuning ratio is nonsensitive to the primary system damping. The values at Table 2 were obtained simply applying (9) and (10). The values at Table 3 were obtained numerically. For simplification purposes, we will assume that (9) is also valid for the FOF PSD.

Table 3: Optimized absorber parameters for FOF noise for different mass ratio and primary system damping

μ (%)	Primary system without damping		Damping of 1%		Damping of 2%		Damping of 5%	
	γ_{opt}	ζ_{opt}	γ_{opt}	ζ_{opt}	γ_{opt}	ζ_{opt}	γ_{opt}	ζ_{opt}
0.5	0.9956	0.0317	0.9946	0.0317	0.9934	0.0317	0.9887	0.0316
1.0	0.9912	0.0448	0.9898	0.0447	0.9883	0.0447	0.9826	0.0446
1.5	0.9868	0.0547	0.9852	0.0547	0.9834	0.0546	0.9769	0.0496
2.0	0.9825	0.0630	0.9807	0.0629	0.9786	0.0629	0.9715	0.0495

3. Random excitation system response using spectral analysis

We are interested in verify the efficacy of the equivalent damping obtained via statistical linearization. A comparison is made by performing spectral analysis of the two methods, namely, the transient response using the nonlinear system and using the frequency response function obtained by the linearized system (equivalent). The two methods are summarized in the diagram shown in Figure 5.

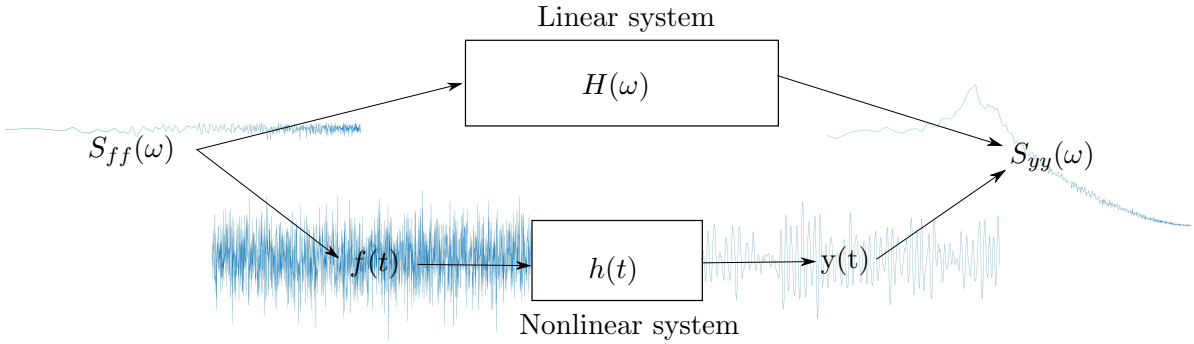

Figure 5: PSD response $S_{yy}(\omega)$ obtained from frequency response function for the linearized case, and from numerical integration for the nonlinear case.

The first method indicated by the bottom path of the diagram starts from choosing the model of PSD $S_{ff}(\omega)$, then one can obtain the random excitation $f(t)$ in the time domain by doing a Fast Fourier Transform (FFT) operation. Next, the displacement $y(t)$ is calculated by solving the equation of motion using 4^{th} order Runge Kutta. The response PSD $S_{yy}(\omega)$ is finally obtained via periodogram [10].

The next method is indicated by the upper path of the diagram. In this case, we used the equivalent damping to obtain the frequency response function $H(\omega)$ and from the forcing PSD we can use one of the most powerful equation from stochastic analysis, $S_{yy} = |H(\omega)|^2 S_{ff}$ [10] to get the response PSD. From this linear system equation one can obtain directly the response spectrum and it is possible to notice that this method is relatively straightforward and require less computational power hence the reason for all the work to find the equivalent damping.

4. Numerical results

Murtagh Basu and Broderick [13, 14] present a simplified model of wind turbine as a cantilever (Figure 6). This simplification is reduced as a one degree of freedom (1DoF) model in Avila et al. [15]. Using structural characteristics of Murtagh Basu and Broderick [13, 14] wind turbine

and reducing to a 1DoF model [15], it is possible to obtain equivalent mass and equivalent stiffness of the tower as follows

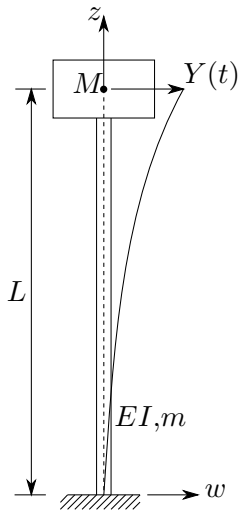

Figure 6: Simplified structural model of wind turbine [15].

$$K^* = \frac{\pi^4}{32L^3} EI, \tag{11}$$

$$M^* = \frac{mL}{2\pi}\left[\pi\left(3 + 2\frac{L_e}{L}\right) - 8\right], \tag{12}$$

where m is the mass per length of the beam and M is the point mass at the top of the beam, w is the normal shift of the beam, E and I are the modulus of elasticity and the moment of inertia respectively. the tower length is L and the equivalent tower length Le is defined as $M = mL_e$.

The wind turbine has a steel tower with 60 m hub height , 3 m width and 0.015 m thickness. The modulus of elasticity is $E = 2.1$ x 10^{11} N/m^2 and density of the steel is $\rho = 7,850$ kg/m^3. The rotor mass is $M = 19,876$ kg. Using these data in (11) and (12) and using the dimensionless parameter length ratio $\alpha = 0.9$ and $\nu = 0.1$, one can obtain $\omega_e = 3.6450$ and $\zeta_e = 0.0018$.

The results presented in Figure 7 illustrate the two methods and the case without the absorber for reference for two input PSD excitation, white noise with $S_0 = 1$ in Figure 7(a) and FOF in 7(b). It can be observed a good approximation between the two methods as well as a good vibration dissipation comparing the case without the TLCD. There is a slightly difference between equivalent and nonlinear models for high frequencies. This difference can be explained by the numerical approximations and do not cause major disturbance in the region of interest, i.e., the resonance peak is outside the area in which that malfunction occurs. Figure 8 shows the PSD response for different mass ratio values in both PSD cases. One may notice a good vibration absorption comparing with the case without TLCD, but there is no significant difference in the change of masses ratio. Physically, it would not be interesting mass ratio greater than $\mu = 0.1$ since the mass of the absorber would be too big and impractical in real applications.

Figure 9 and Figure 10 illustrate the evolution in time of the structure displacement for different values of mass ratio μ when subjected input PSD excitation, white noise and FOF, respectively. For white noise PSD excitation shown in Figure 9 there was a reduction in the mean squared displacement of the main structure when the TLCD was added by 3.46% for $\mu = 0.05$ and 5.45% for $\mu = 0.1$. For the FOF PSD excitation shown in Figure 10, the displacement value

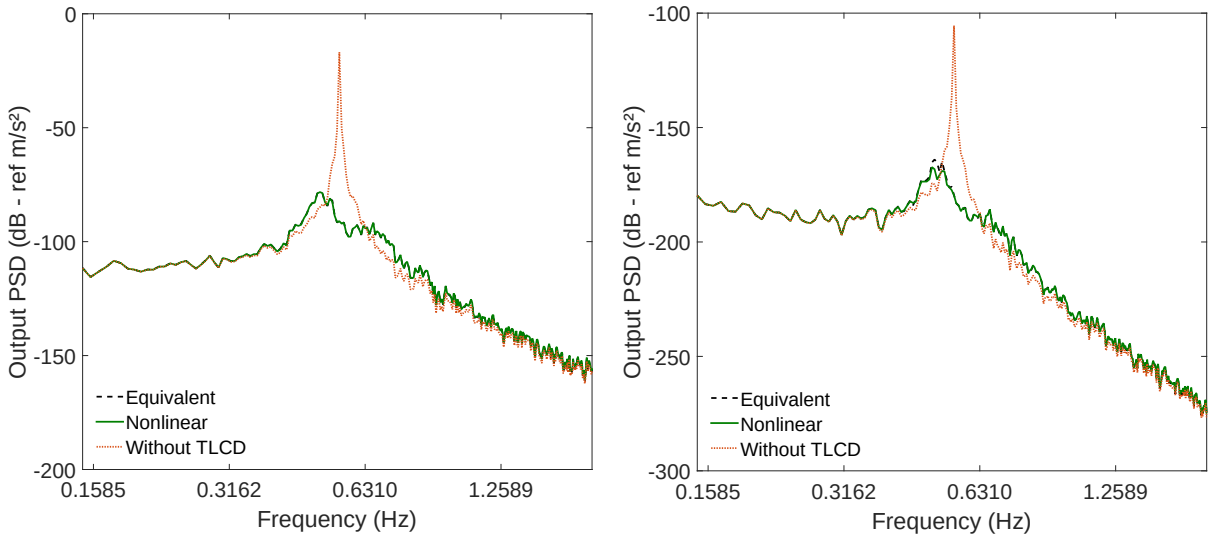

Figure 7: PSD of main system response to (a) white noise and (b) FOF random excitation without and with TLCD, obtained via statistical linearization and via numerical integration of nonlinear system.

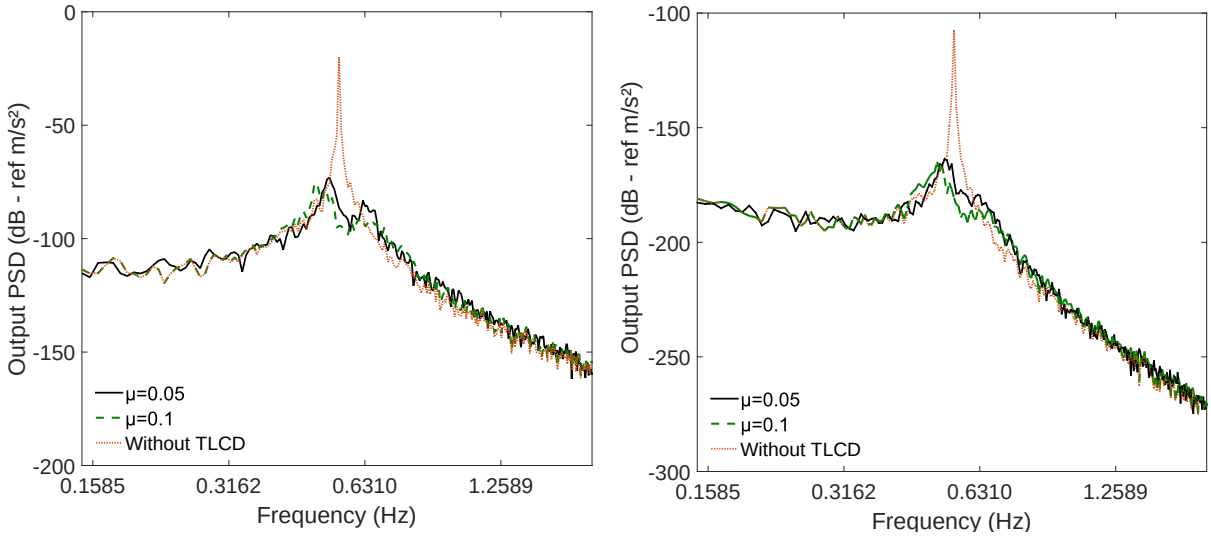

Figure 8: PSD of main system to (a) white noise random excitation and (b) FOF without and with TLCD for different mass ratio.

does not change significantly between the two mass ratio. There was a reduction of 11.48% for $\mu = 0.05$ and 11.49% for $\mu = 0.1$.

5. Final remarks

This work focus on passive tuned liquid column damper with application on wind turbines. The use of absorber devices as means of vibration mitigating in wind turbines has grown in number

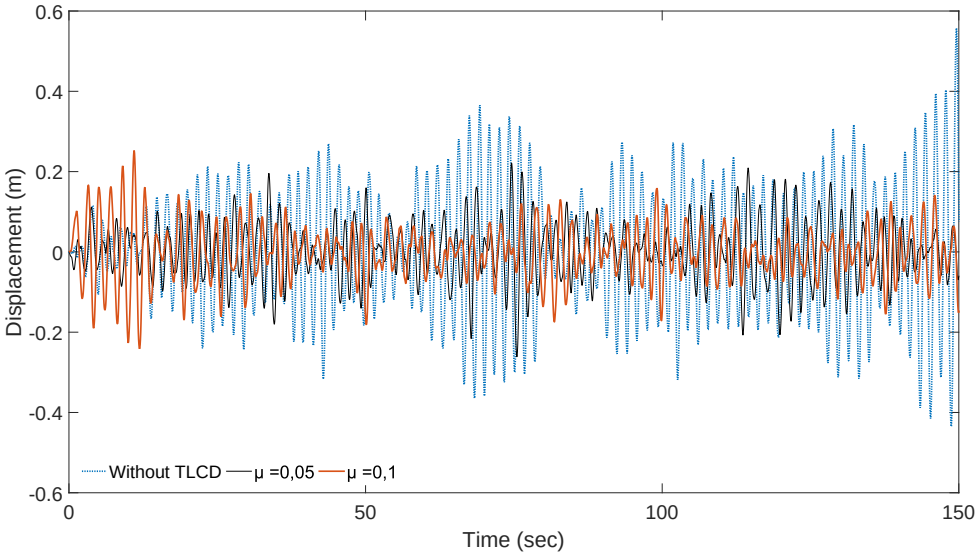

Figure 9: Temporal evolution of structural displacement for different values of the mass ratio μ subjected to white noise.

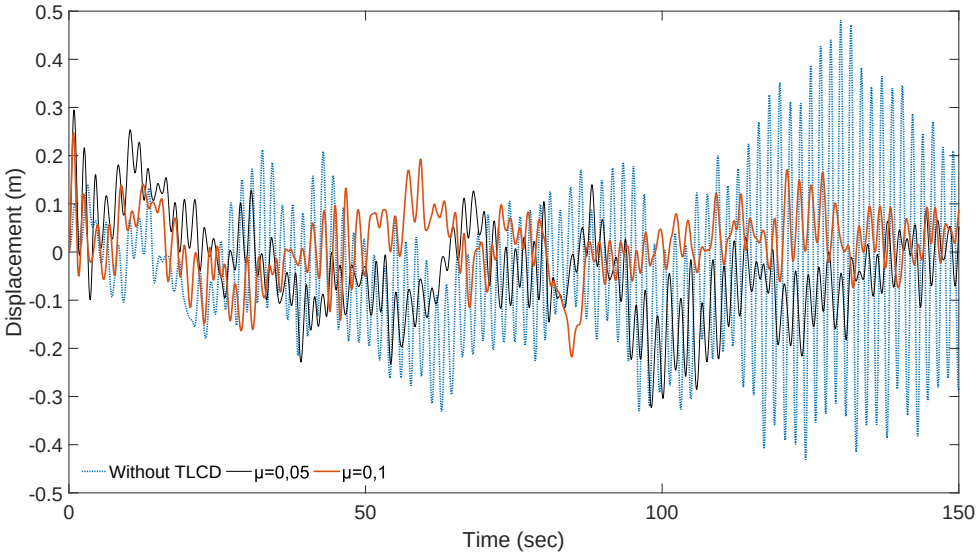

Figure 10: Temporal evolution of structural displacement for different values of the mass ratio μ subjected to FOF.

in recent years. Among the variety of existing devices, it was decided to explore the TLCD due to its relatively low cost and good efficiency.

The proposed analysis aimed to compare the nonlinear model with the equivalent linearized system as well as to verify the efficacy of the TLCD using two types of excitation, white noise filter and first order filter. The comparison between the linear and nonlinear model was presented using spectral analysis. The result obtained demonstrated good approximation between the two and the linearized method can be used without many concerns. Furthermore, the TLCD showed

good energy dissipation with both white noise PSD, and FOF PSD random excitation. The latter featured more satisfactory results as it best describe the wind loads.

Finally, the TLCD showed a significant energy dissipation of the primary structure by reducing the displacement between 3 to 11%. The results for the influence in the dissipation of energy based on the variation of mass ratio did not show considerable changes, consequently, it is more sensible to use the least possible mass for the device since it would have a smaller impact on the total weight of the structure.

Further work is needed to validate the robustness of the model which include experimental validation, use of other PSDs such as the ones discussed in this paper and finally, a more detail analysis of the wind turbine model considering the complexity of its geometry and more degrees of freedom.

6. Acknowledgments

The authors would like to thank the CNPq and MCTI for the financial support (Process number 406895/2013-9).

References

[1] Amarante O A, Brower M and Zack J 2001 (Ministerio de Minas e Energia e Eletrobras)
[2] Zuluaga A L 2007 Master's thesis University of Brasilia
[3] Lima D V F 2009 Master's thesis University of Brasilia
[4] Valencia L 2009 Master's thesis University of Brasilia
[5] Colwell S and Basu B 2009 *Engineering Structures* **31** 358–368
[6] Lackner M A and Rotea M A 2011 *Mechatronics* **21** 704–719
[7] Farshidianfar A 2011 *6th National Congress on Civil Engineering, 6NCCE*
[8] Roberts J B and Spanos P D 2003 *Random vibration and statistical linearization* (Courier Corporation)
[9] Yalla S K and Kareem A 2000 *Journal of Structural Engineering* **126** 906–915
[10] Newland D E 2012 *An introduction to random vibrations, spectral & wavelet analysis* (Courier Corporation)
[11] Kaasen K E *et al.* 1999 *The Ninth International Offshore and Polar Engineering Conference* (International Society of Offshore and Polar Engineers)
[12] Thráinsson H, Kiremidjian A S and Winterstein S R 2000 *Modeling of earthquake ground motion in the frequency domain* (John A. Blume Earthquake Engineering Center)
[13] Murtagh P, Basu B and Broderick B 2004 *Computers & structures* **82** 1745–1750
[14] Murtagh P, Basu B and Broderick B 2005 *Engineering structures* **27** 1209–1219
[15] Avila S M, Barcelos M, Morais M V G, Shzu M A M and Silva R C 2009 *20th International Congress of Mechanical Engineering COBEM*